Physics of Plasmas

On kinetic electrostatic plasma waves carrying orbital angular momentum

Cite as: Phys. Plasmas **28**, 074507 (2021); https://doi.org/10.1063/5.0040579
Submitted: 14 December 2020 • Accepted: 06 July 2021 • Published Online: 21 July 2021

S. A. Khan and A. Fukuyama

View Online
Export Citation
CrossMark

ARTICLES YOU MAY BE INTERESTED IN

A kinetic model of friction in strongly coupled strongly magnetized plasmas
Physics of Plasmas **28**, 072107 (2021); https://doi.org/10.1063/5.0054552

A particle-in-cell code comparison for ion acceleration: EPOCH, LSP, and WarpX
Physics of Plasmas **28**, 074505 (2021); https://doi.org/10.1063/5.0053109

Electron holes in a κ distribution background with singularities
Physics of Plasmas **28**, 072110 (2021); https://doi.org/10.1063/5.0059613

AIP Publishing

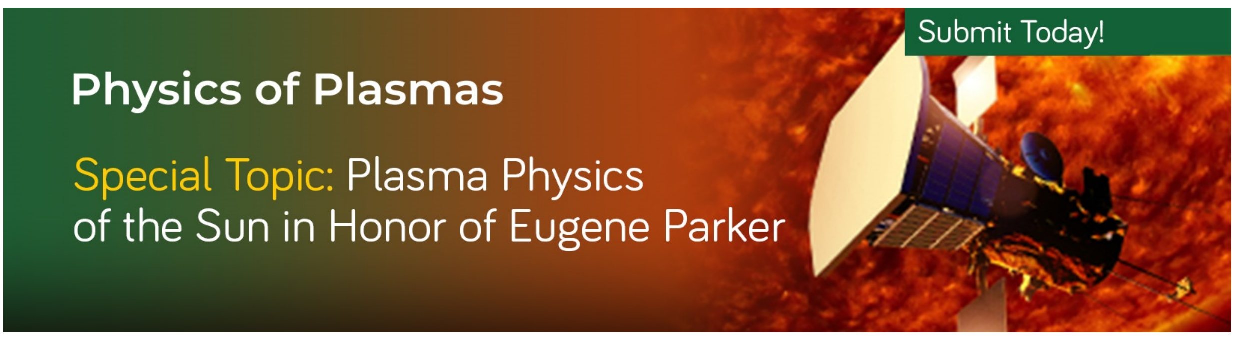

© 2021 Author(s).

On kinetic electrostatic plasma waves carrying orbital angular momentum

Cite as: Phys. Plasmas **28**, 074507 (2021); doi: 10.1063/5.0040579
Submitted: 14 December 2020 · Accepted: 6 July 2021 ·
Published Online: 21 July 2021

View Online Export Citation CrossMark

S. A. Khan[1,a] and A. Fukuyama[2]

AFFILIATIONS

[1]National Centre for Physics, Quaid-i-Azam University Campus, Islamabad 45320, Pakistan
[2]Department of Nuclear Engineering, Kyoto University, Kyoto 615-8540, Japan

[a]Author to whom correspondence should be addressed: sakhan@ncp.edu.pk

ABSTRACT

A kinetic description of electron plasma waves carrying orbital angular momentum is revisited by introducing a variable transformation, which confirms a more natural representation of wave propagation in electron–ion plasma extendable to an electron–positron plasma. Specifically, the twisted Landau resonance condition is expressed in a consistent way, which expands the resonance region, and hence modifies the usual assumption of decomposition of the susceptibility in axial and poloidal components involving two separate poles. The present formulation is recommended by numerical analysis and comparison with typical results and illustrations.

Published under an exclusive license by AIP Publishing. https://doi.org/10.1063/5.0040579

It has been known for a long time that photon beams can carry an orbital angular momentum (OAM) associated with the spatial distribution of the beam intensity and phase of the optical field, even at the single-photon level.[1] This is in addition to the well-demonstrated intrinsic spin angular momentum arising due to wave polarization.[2] The photon OAM provides a fundamentally new degree of freedom, which has led to novel vortex beam sources including chiral light,[3] electron and magnon beams,[4,5] and corkscrew lasers for terabit-scale data transfer.[6] It is now well understood that collimated electromagnetic beams exhibiting helical profile with an azimuthal component of Poynting vector can be mathematically presented by an orthonormal set of Laguerre–Gaussian (LG) functions. In optics, these are eigenfunctions of the paraxial equation and provide a natural basis for modeling of beam dynamics. Realizing the fact that optical beams with OAM are able to excite twisted density perturbations, Mendonca and co-workers have theoretically explained the exchange of OAM between electromagnetic and electrostatic waves in a plasma.[7] Pumping the plasma with a collimated laser beam described by LG functions leads to twisted acoustic and Langmuir modes owing to stimulated Brillouin scattering (SBS) and stimulated Raman scattering (SRS) processes, respectively. The idea has opened the door for subsequent studies including new investigations on waves and instabilities.[8–11] The LG beams introduce nontrivial effects in the plasma due to intertwined helical wavefronts, for instance, magnetic and Alfvenic tornadoes,[12,13] twisted plasma accelerator,[14] ring-shaped morphology of plasma turbulence in radio-pumping,[15] twisted photon emission at single electron level,[16] and so on.

In the studies of twisted beam–plasma interactions, wave–particle phenomena are essential in wave mixing, particle acceleration, and nonlinear decay of laser beams with OAM for which a kinetic framework is required.[7,17] These processes are particularly important for the excitation and damping of twisted plasmons to demonstrate the influence of OAM states. Kinetic theory of electron plasma waves with OAM was presented by Mendonca for the first time in cylindrical geometry under the paraxial approximation.[17] The model explained the dispersion and damping properties of the twisted plasmons and implemented in subsequent studies of electron and ion kinetic modes.[18,19] The description is formally similar to the plane wave case with an important difference in the Landau damping condition due to the contribution of new resonances. However, due to the decomposition of the imaginary part of the susceptibility into axial and poloidal parts, the integration over the velocity space was restricted to a resonance line in the (v_θ, v_z) plane involving two separate poles expressed by two delta functions. A more consistent description with a broader scope is necessary to aid in the understanding of wave–particle interactions and OAM states associated with twisted plasma waves. In a recent study in this context, Blackman *et al.* have described the structure of twisted kinetic plasma wave by including the mutual coupling of the modes with different radial and azimuthal wavenumbers in the paraxial approximation.[20] The mode coupling is dealt with by using an expansion of the paraxial parameter, which is the ratio of plasma wavelength and the radial width of the wave packet. For weak coupling and small wave number, plasmon dispersion and damping are discussed.

Published under an exclusive license by AIP Publishing

In this brief communication, the theoretical model of Ref. 17 is revisited by adopting a generalized formulation based on a variable transformation. This enables one to derive the dielectric function and express the wave propagation in a more natural way. Specifically, we show that the imaginary part of the dielectric function can be evaluated involving only one pole including the axial motion, and a poloidal contribution, carrying finite OAM. By using an arbitrary mass parameter, the twisted wave motion in an electron–ion plasma can be extended to an electron–positron plasma. It is worth noting that interacting LG beams introduce novel excitations in electron–positron plasmas.[21,22] Stable and relatively denser ($10^{16}\,\mathrm{cm}^{-3}$) laser-produced electron–positron plasmas have been demonstrated in the laboratory,[23] thereby providing a path for studying collective behavior of electrons and positrons.[24]

Let us consider a small amplitude wave in a two-species plasma described by the electrostatic potential V and the species ($s = i, e$) distribution function $f_s(\mathbf{r}, \mathbf{v}, t)$, where the potential satisfies the Poisson's equation

$$\nabla^2 V = -4\pi \sum_s q_s \int \tilde{f}_s d\mathbf{v}, \tag{1}$$

and the evolution of distribution function is expressed by the Vlasov equation

$$\left(\frac{\partial}{\partial t} + \mathbf{v}\cdot\nabla\right)\tilde{f}_s + \frac{q_s}{m_s}\mathbf{E}\cdot\frac{\partial f_{s0}}{\partial \mathbf{v}} = 0, \tag{2}$$

with q_s the species charge ($q_e = -e$ and $q_i = e$), and tilde (0) the perturbation (equilibrium). The electrostatic field $\mathbf{E} = -\nabla V$, and the potential V is related to the deviation of the distribution function $\tilde{f}_s = f_s - f_{s0}$ from the Maxwellian distribution at equilibrium

$$f_{s0}(\mathbf{r}, \mathbf{v}, t) = \frac{n_{s0}}{(2\pi T_s/m_s)^{3/2}} \exp\left(-m_s \mathbf{v}^2/2T_s\right), \tag{3}$$

where n_{s0} and T_s are the species equilibrium density and temperature in energy units, respectively. The wave propagating along z-axis is assumed to be evolving as $\exp(ikz)$ with slowly changing amplitude, which leads to $\nabla^2 V \simeq (\nabla_\perp^2 - k^2 + 2ik\,\partial/\partial z)V$. The potential V associated with waves carrying OAM satisfies the paraxial equation

$$\left(\nabla_\perp^2 + 2ik\frac{\partial}{\partial z}\right)V = 0. \tag{4}$$

Such a condition reduces the Poisson's Eq. (1) to

$$k^2 V = 4\pi \sum_s q_s \int \tilde{f}_s(\mathbf{v}) d\mathbf{v}. \tag{5}$$

The solution to this equation in cylindrical coordinates can be given as a superposition of LG modes, such that

$$V(\mathbf{r}, t) = \sum_{p,l} \tilde{V}_{p,l} F_{p,l}(r, z) \exp(il\theta) \exp(ikz - i\omega t), \tag{6}$$

where $\tilde{V}_{p,l}$ are the mode amplitudes; θ is the azimuthal angle; $p \geq 0$ is an integer, which denotes radial mode; and l is positive or negative angular mode number, which enumerates the OAM. The LG mode function $F_{p,l}(r, z)$ is given by

$$F_{p,l}(r, z) = C_{pl} X^{|l|} L_p^{|l|}(X) \exp(-X/2), \tag{7}$$

where $X = r^2/w^2(z)$, $w(z)$ is the wave beam waist, and $C_{p,l}$ is a normalization factor denoted by

$$C_{p,l} = \frac{1}{2\sqrt{\pi}} \sqrt{\frac{(l+p)!}{p!}}. \tag{8}$$

A generalized or associated Laguerre polynomial $L_p^{|l|}(X)$ of degree p and l is defined by the Rodrigues formula

$$L_p^{|l|}(X) = \frac{\exp(X)}{p! X^{|l|}} \frac{d^p}{dX^p}\left[X^{|l|+p} \exp(-X)\right]. \tag{9}$$

The set of functions $F_{p,l}$ is orthogonal and normalized according to the relation

$$\int_0^\infty r dr \int_0^{2\pi} d\theta F_{p,l} F_{p',l'} \exp\left[i(l'-l)\theta\right] = \delta_{p,p'}\delta_{l,l'}, \tag{10}$$

where $\delta_{p,p'}, \delta_{l,l'}$ are the Kronecker symbols. To solve the Eqs. (2) and (5), we need to express the perturbed distribution function in terms of LG modes similar to Eq. (6) as

$$\tilde{f}_s = \sum_{pl} \tilde{f}_{p,l} F_{p,l}(r, z) \exp(il\theta) \exp(ikz - i\omega t). \tag{11}$$

Taking the orthogonality conditions of LG modes into account, the result is an algebraic expression relating the perturbed distribution function $\tilde{f}_{p,l}$ to the potential amplitude $\tilde{V}_{p,l}$ by

$$\tilde{f}_{p,l} = \frac{q_s}{m_s} \frac{\mathbf{q}_{eff}\cdot\partial f_{s0}/\partial\mathbf{v}}{\omega - \mathbf{q}_{eff}\cdot\mathbf{v}} \tilde{V}_{p,l}, \tag{12}$$

where

$$\mathbf{q}_{eff} = -iq_r\hat{\mathbf{e}}_r + lq_\theta\hat{\mathbf{e}}_\theta + (k - iq_z)\hat{\mathbf{e}}_z, \tag{13}$$

which is independent of r. Here, $q_\theta = \int_0^\infty F_{p,l}^2 dr$ and $q_j = \int_0^\infty F_{p,l}\frac{\partial F_{p,l}}{\partial j} r dr$ for $j = r, z$. The kinetic dispersion relation can thus be obtained in a way similar to the conventional representation of the dielectric function

$$\epsilon(\omega, \mathbf{q}_{eff}) = 1 + \sum_s \chi_s(\omega, \mathbf{q}_{eff}), \tag{14}$$

with susceptibilities defined by

$$\chi_s(\omega, \mathbf{q}_{eff}) = \frac{\omega_{ps}^2}{k^2} \int \frac{\mathbf{q}_{eff}\cdot\partial f_{s0}/\partial\mathbf{v}}{\omega - \mathbf{q}_{eff}\cdot\mathbf{v}} d\mathbf{v}, \tag{15}$$

which resembles the plane wave case but different in dependencies. The Landau resonance condition in Eq. (15) is modified, and the resonance frequency is given explicitly by $\omega = kv_z + lq_\theta v_\theta - i(q_r v_r + q_z v_z)$. The significance of the resonances can be seen in the limit $|q_r|, |q_z| \ll |lq_\theta|$, which leads to $\omega = kv_z + lq_\theta v_\theta$, a form having a poloidal contribution in the resonance frequency. Then, the dielectric function including the azimuthal term yields

$$\epsilon(\omega, k, lq_\theta) = 1 + \sum_s \frac{\omega_{ps}^2}{k^2} \int \left(\frac{k\partial f_{s0}/\partial v_z + lq_\theta \partial f_{s0}/\partial v_\theta}{\omega - kv_z - lq_\theta v_\theta}\right) d\mathbf{v}, \tag{16}$$

Published under an exclusive license by AIP Publishing

and the integral can be evaluated over v_z and v_θ in the plane (v_z, v_θ). We use the general expression (16) to obtain the dispersion properties of twisted electrostatic modes in an electron–ion plasma and also in an electron–positron plasma due to the straightforward extension. However, unlike those of an electron–ion plasma, the longitudinal waves in a mass-symmetric electron–positron plasma cannot be separated by species due to their simultaneous equilibrium state. Instead of an electron plasma wave driven by the electron number density and an acoustic wave governed primarily by the ion motion, we have a plasma wave associated with a difference in electron and positron density fluctuations $(n_e - n_p)$ and an acoustic wave described by the sum of the total density fluctuations $(n_e + n_p)$,[25,26] so it is plausible to define an arbitrary mass parameter

$$\beta = \frac{m_e}{m_+}\begin{cases} = 1 & \text{for e-p plasma,} \\ \ll 1 & \text{for e-i plasma,} \end{cases} \tag{17}$$

such that the dielectric function can connect a dispersion relation in heavy-ion and electron–positron limits by changing β ("+" denotes ions or positrons). We can then write Eq. (16) as

$$\epsilon(\omega, k, lq_\theta) = 1 + (1+\beta)\frac{\omega_{pe}^2}{k^2}\int \frac{\mathcal{F}(v_z, v_\theta)}{\omega - kv_z - lq_\theta v_\theta} d\mathbf{v}, \tag{18}$$

where

$$\mathcal{F}(v_z, v_\theta) = k\frac{\partial f_{e0}}{\partial v_z} + lq_\theta \frac{\partial f_{e0}}{\partial v_\theta}, \tag{19}$$

and f_{e0} is the isotropic electron distribution function at equilibrium. One can find the Langmuir mode dispersion in an electron–ion plasma for $\beta = 0$, and an electron–positron plasma having equal species temperature for $\beta = 1$. The ion-acoustic mode includes the ion contribution and propagates with phase velocity much smaller than the electron thermal velocity but much larger than the ion thermal velocity for $T_e \gg T_i$. In the present case, the ion-acoustic mode calculation is not included.

To derive the dispersion and damping properties of the twisted Langmuir mode in a Maxwellian plasma obeying the distribution function (3), let us introduce the variable transformation,

$$\xi = v_z + \frac{lq_\theta}{k}v_\theta, \quad \eta = v_\theta - \frac{k}{lq_\theta}v_z, \tag{20}$$

resulting in

$$v_z = \frac{\xi}{2} - \frac{\sigma\eta}{2}, \quad v_\theta = \frac{\eta}{2} + \frac{\xi}{2\sigma}, \tag{21}$$

and the Jacobian

$$J = \frac{\partial(v_z, v_\theta)}{\partial(\xi, \eta)} = \frac{1}{2}, \tag{22}$$

where $\sigma = lq_\theta/k$ is the parameter characterizing the OAM. This procedure allows us to write the electron susceptibility from Eq. (18) as

$$\chi_e(\omega) = \frac{\omega_{pe}^2}{2k^2}\int \frac{\mathcal{F}(\xi, \eta)}{\omega - k\xi} d\xi d\eta dv_r, \tag{23}$$

where

$$\mathcal{F}(\xi,\eta) = \frac{1}{(2\pi)^{3/2}}\frac{k\xi}{v_{Te}^3}\exp\left[-\frac{1}{2v_{Te}^2}\left\{\left(\frac{\xi}{2} - \frac{\sigma\eta}{2}\right)^2 + \left(\frac{\eta}{2} + \frac{\xi}{2\sigma}\right)^2 + v_r^2\right\}\right], \tag{24}$$

and $v_{Te} = (T_e/m_e)^{1/2}$. By reordering the argument of the exponential function and integrating over v_r and $\eta + (1-\sigma^2)/\sigma(1+\sigma^2)\xi$, we obtain

$$\chi_e(\omega) = \frac{\omega_{pe}^2}{k^3 v_{Te}^3}\frac{1}{(2\pi)^{1/2}}\frac{1}{(1+\sigma^2)^{1/2}}\int d\xi \frac{k\xi}{\xi - \omega/k}\exp\left[-\frac{\xi^2}{2v_{Te}^2(1+\sigma^2)}\right]. \tag{25}$$

The denominator term of the transformed integral in (25); $\xi - \omega/k$, looks similar to a formal representation of the plane wave, $v_z - \omega/k$, in which $k = \sqrt{\mathbf{k}\cdot\mathbf{k}}$ and $v_z = \mathbf{k}\cdot\mathbf{v}/k$. Thus, the resonant denominator can be treated by the Plemelj formula

$$\frac{\xi}{\xi - \omega/k} = \mathscr{P}\left\{\frac{\xi}{\xi - \omega/k}\right\} + i\pi\,\xi\,\delta(\xi - \omega/k), \tag{26}$$

to obtain an expression using the plasma dispersion function

$$\chi_e(\omega) = \frac{\omega_{pe}^2\omega}{\sqrt{2}\sqrt{1+\sigma^2}k^3 v_{Te}^3} Z\left(\frac{\omega}{\sqrt{2}\sqrt{1+\sigma^2}kv_{Te}}\right), \tag{27}$$

where the plasma dispersion function $Z(\zeta)$ is defined by

$$Z(\zeta) = \frac{1}{\sqrt{\pi}}\int_{-\infty}^{\infty} \mathrm{d}\xi \frac{1}{\xi - \zeta}\exp(-\xi^2). \tag{28}$$

For rigorous analysis, we numerically solve the dispersion relation

$$\epsilon(\omega) = 1 + \chi_e(\omega) = 0, \tag{29}$$

by using the two-dimensional Newton method for complex function. We recall that $\epsilon(\omega)$ is a complex quantity and solution of the system is also complex, in general, consisting of real and imaginary parts of the frequency, $\omega = \omega_r + i\gamma$.

As an approximation for small wave number, $|kv_{Te}/\omega| \ll 1$, Eq. (27) reduces to the following relation for the complex susceptibility

$$\begin{aligned}\chi_e(\omega) = &-\frac{\omega_{pe}^2(1+\sigma^2)}{\omega^2}\left(1 + \frac{3(1+\sigma^2)k^2 v_{Te}^2}{\omega^2} + \cdots\right) \\ &+ i\frac{\omega}{kv_{Te}}\frac{1}{k^2\lambda_{De}^2(1+\sigma^2)^{1/2}}\sqrt{\frac{\pi}{2}}\exp\left[-\frac{\omega^2}{2k^2 v_{Te}^2(1+\sigma^2)}\right],\end{aligned} \tag{30}$$

where $\lambda_{De} = v_{Te}/\omega_{pe}$. Thus, one obtains for wave dispersion,

$$\omega_r^2 = \omega_{pe}^2(1+\sigma^2)\left[1 + 3k^2\lambda_{De}^2\right], \tag{31}$$

and for the imaginary part,

$$\gamma = -\sqrt{\frac{\pi}{8}}\frac{\omega_r^4}{k^3 v_{Te}^3(1+\sigma^2)^{3/2}}\exp\left[-\frac{1}{(1+\sigma^2)}\frac{\omega_r^2}{2k^2 v_{Te}^2}\right], \tag{32}$$

which shows that the poloidal velocity (v_θ) term introduces an additive contribution of orbital angular momentum to the axial parameter, a correction to the usual plasmon dispersion. The relative wave damping including thermal correction can be written as

Published under an exclusive license by AIP Publishing

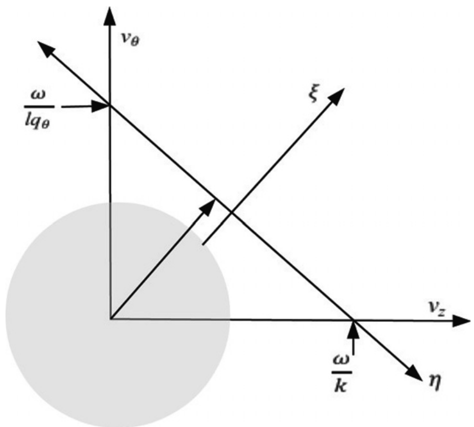

FIG. 1. The modified Landau resonance region defined in the $(v_z, v_\theta,)$ plane after variable transformation.

$$\frac{\gamma}{\omega_{pe}} = -\sqrt{\frac{\pi}{8}}\frac{(1+\sigma^2)^{1/2}}{k^3\lambda_{De}^3}\left(1+3k^2\lambda_{De}^2\right)^2\exp\left[-\frac{\left(1+3k^2\lambda_{De}^2\right)}{2k^2\lambda_{De}^2}\right]. \tag{33}$$

It is worth noting that the imaginary part of the integral in Eq. (23) is evaluated for $\xi \to \omega/k$, involving only one delta function, viz., $\delta(\omega - k\xi) = (-1/k)\delta(\xi - \omega/k)$. Hence, pole contribution in the present formulation is included in terms of the transformed variable ξ instead of decomposition of the velocity integral in z- and θ-dependent parts by defining the respective velocity variables, $u_z = u_z(v_\theta)$ and $u_\theta = u_\theta(v_z)$, to determine the two separate poles explicitly, as in Ref. 17. Both the poles are indeed the same. In this way, restriction of integration over the resonance line in the plane (v_z, v_θ) defined by two delta functions is removed and the integration space is extended as illustrated in Fig. 1. The Landau resonance is shifted with respect to the axial phase velocity due to the transverse structure of the plasma wave owing to the poloidal velocity term.

The dielectric function [Eq. (18)] leads to an electron–positron plasma by setting $\beta = 1$. In this case, the response time of electrons and positrons to density perturbations for $m_+ = m_e$ and $T_+ = T_e$ is equal. The wave dispersion and damping rate are similar to the Langmuir wave in electron–ion plasma except for a small difference

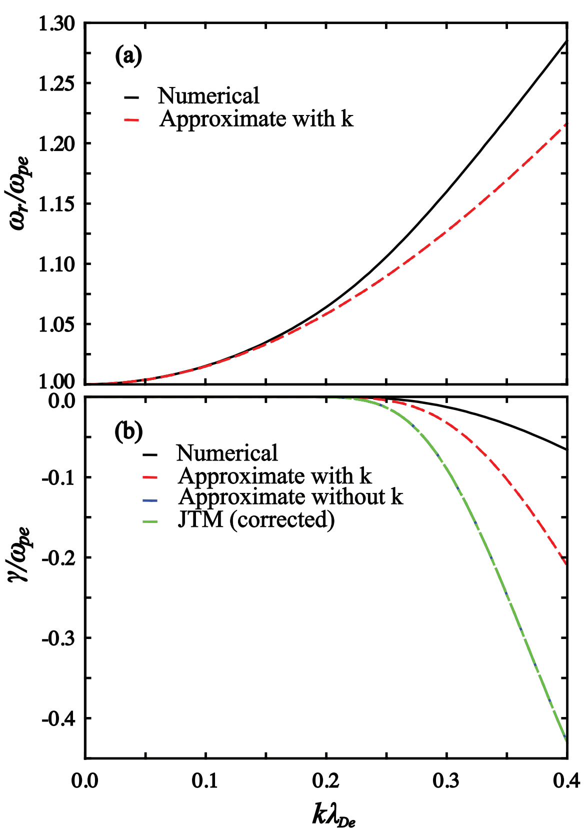

FIG. 2. Variation of wave frequency (upper panel) and damping rate (lower panel) is shown as a function of axial wavelength $(k\lambda_{De})$ for $\sigma = 0.0$. Numerical solution is represented by solid black curve, whereas approximate solution with (without) k-dependence is shown by dashed (long dashed) red (blue) curve. The green (double dashed) curve represents the result of Ref. 17 (JTM) including correction.

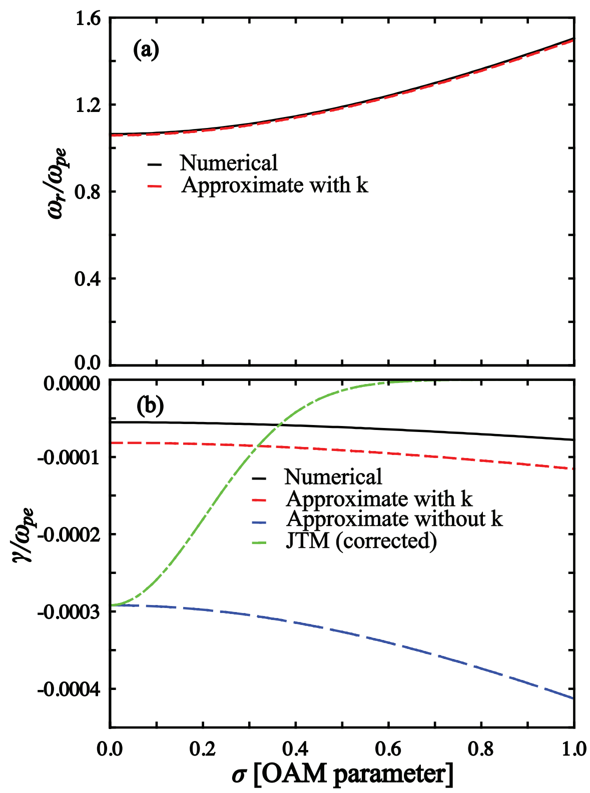

FIG. 3. Wave frequency (upper panel) and damping rate (lower panel) is shown as a function of the OAM parameter $\sigma = lq_\theta/k$ with $k\lambda_{De} = 0.2$ where representation of the solutions is similar to Fig. 2.

Published under an exclusive license by AIP Publishing

in the definition of "plasma frequency," which can be written as "$\omega_p = \sqrt{2}\omega_{pe}$," and the Debye length as "$\lambda_D = v_{Te}/\omega_p$."

Having described the analytical formulation and approximate solution for small wave number, we perform a detailed analysis by numerically solving the dispersion relation with no limitation on the relation between ω and kv_{Te}. The features of wave propagation are described for arbitrary parameters with a comparison of our formulation with the model of J. T. Mendonca (JTM).[17] It was noticed that the contribution of the OAM parameter to the dispersion relation attributed to the factor $\partial\epsilon_r(\omega)/\partial\omega$ is missing in the wave damping relation of Ref. 17, which modifies the real frequency even in the absence of thermal correction, $\omega_r = \omega_{pe}(1+\sigma^2)^{1/2}$. Its inclusion reduces Eq. (30) of Ref. 17 to

$$\frac{\gamma}{\omega_{pe}} = -\sqrt{\frac{\pi}{8}}\frac{(1+\sigma^2)}{k^3\lambda_{De}^3}\left\{\exp\left[-\frac{(1+\sigma^2)}{2k^2\lambda_{De}^2}\right]\exp\left[-\frac{\sigma^2}{2}\right] + \frac{1}{\sigma}\exp\left[-\frac{(1+\sigma^2)}{2\sigma^2k^2\lambda_{De}^2}\right]\exp\left[-\frac{1}{2\sigma^2}\right]\right\}, \tag{34}$$

which is also compared with the results of the present formulation in numerical analysis. Numerical solution of the dispersion relation $\epsilon(\omega) = 1 + \chi_e(\omega) = 0$ with Eq. (27) and the approximate solution including k-dependence, Eq. (33), are shown by solid (black) and dashed (red) curves, respectively, as in Figs. 2 and 3. Figure 2 shows k-dependence of real frequency (a) and damping rate (b), and comparison with approximate values for $\sigma = 0$. The damping amplitude without k-dependence is larger (long dashed blue curve) and coincides with the proposed modified result of Ref. 17 represented by a double dashed (green) curve. In Fig. 3, wave frequency (a) and damping rate (b) are shown as a function of the OAM parameter σ for $k = 0.2$. The exact and approximate solutions for ω_r are very close to each other. Comparison of damping rate without k-dependence is shown by the lowest long dashed (blue) curve in Fig. 3(b) trending significantly different from the case of Ref. 17 for increasing σ. Parameter dependence of the numerical solution is shown in Figs. 4 and 5. Figure 4 shows the axial wavelength ($k\lambda_{De}$) dependence for $\sigma = 0.0$, 0.4, 0.8, 1.2, 1.6, and 2.0, whereas Fig. 5 shows σ-dependence for $k\lambda_{De} = 0.0$, 0.4, 0.8, 1.2, 1.6, and 2.0, starting from below in (a) and above in (b). The dependencies of real frequency and Landau damping rates are further elaborated by contour plots in Fig. 6, where $\omega_r/\omega_{pe} = 1.0$ at $k\lambda_{De} = \sigma = 0$, $\gamma/\omega_{pe} = 0.0$ for $k\lambda_{De} = 0$, and all contours are separated by equal steps of 0.5. The numerical results show that the proposed formulation has an advantage of the smoother analysis of twisted plasma wave through a more natural description with an extended resonance region.

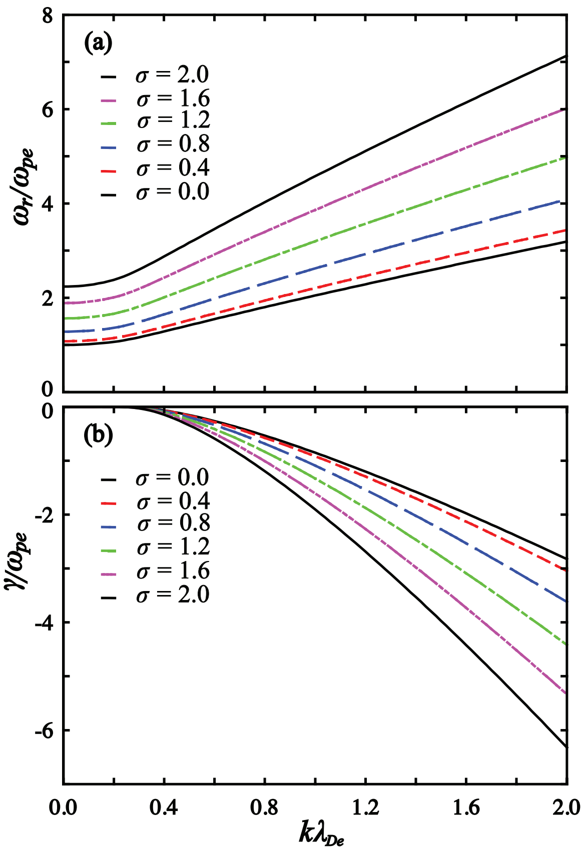

FIG. 4. Numerical result showing the change of frequency (upper panel) and relative Landau damping (lower panel) with various σ, as a function of axial wavelength starting from below in (a) and above in (b).

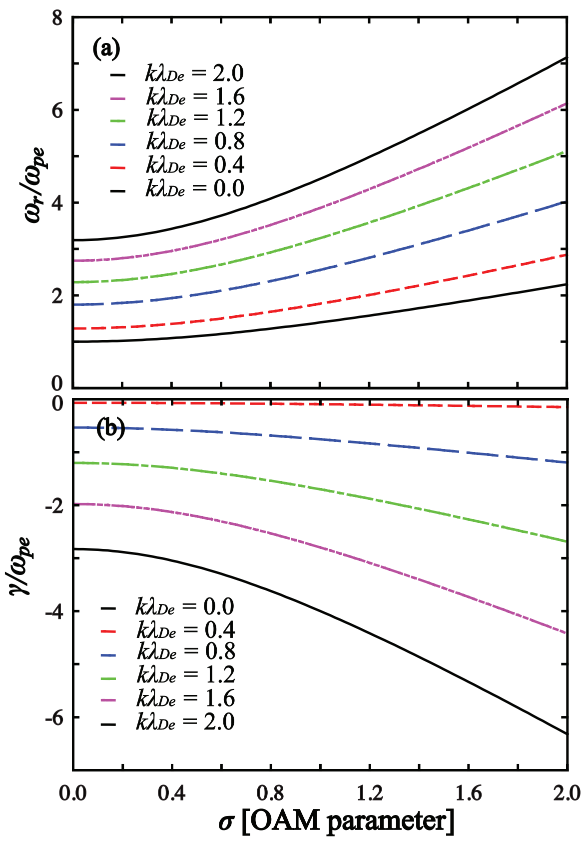

FIG. 5. Change of frequency (upper panel) and relative Landau damping (lower panel) is shown for various axial wavelength dependencies as a function of σ.

Published under an exclusive license by AIP Publishing

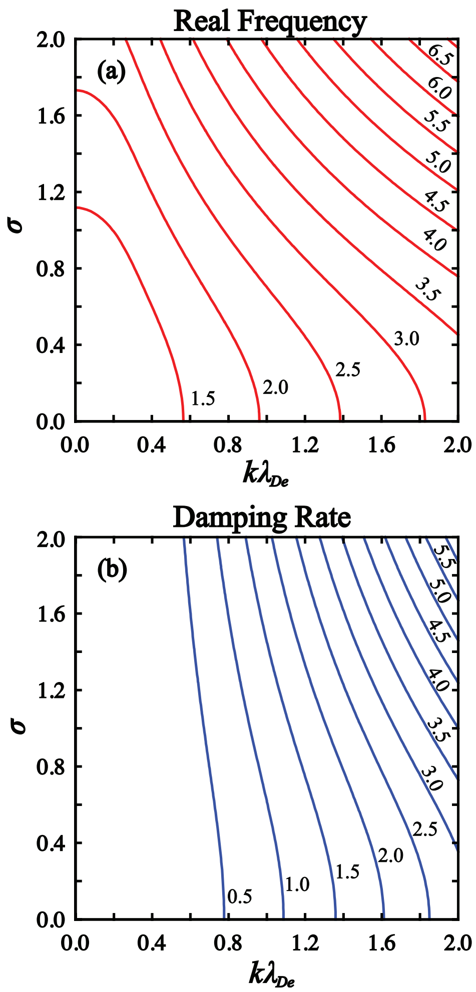

FIG. 6. Numerical results of twisted Langmuir mode are presented as contour maps with upper panel showing the real frequency and lower panel the Landau damping rate with $\omega_r/\omega_{pe} = 1.0$ at $k\lambda_{De} = \sigma = 0$ (a) and $\gamma/\omega_{pe} = 0.0$ for $k\lambda_{De} = 0$ (b). All contours are separated equally by a step of 0.5.

In the recent study presented in Ref. 20, the analytical formulation of twisted kinetic plasma wave considers mutual coupling of the modes with different radial and azimuthal wavenumbers in the paraxial approximation. Strong dependence of coupling between neighboring orbital modes on beam size is assumed. The coupling coefficient, which gives rise to OAM corrections to the wave dispersion and damping [Eqs. (30) and (31)], is attributed to the Gouy phase and curvature terms in the LG functions. The OAM corrections to the dispersion and damping are included for weak coupling case with nonzero λ_{De}/w_b in the limit of $\omega \gg kv_{Te}$, where w_b is the beam radius. For very wide beams, the OAM correction terms vanish and standard expressions for dispersion and damping of plane Langmuir wave are obtained. To this end, the present analysis utilizes the kinetic model for relatively wider beam solutions for arbitrary wave number imposing no limitation on the relation between ω and kv_{Te}. The susceptibility [Eq. (15)] is considered as a function of an effective wave vector $\mathbf{q}_{eff}$ [Eq. (13)] containing an azimuthal term lq_θ. This poloidal contribution in the resonance frequency leads to a nonzero OAM correction term in the plasma wave dispersion and damping [Eqs. (31) and (32)]. Since the mode coupling is not taken into account ($\lambda_{De}/w_b = 0$), the dependence of OAM on beam size does not appear like the case of Ref. 20. Instead, the poloidal velocity term introduces an additive contribution of the OAM to the axial parameter. The plane wave result is reduced in the vanishing σ limit. This may be roughly equivalent to a very wide beam case in a way if $q_\theta \propto 1/w_b$. Yet, a true relation is hard to develop due to the difference in approaches in both papers. Extension of the kinetic analysis for arbitrary wave number including mode coupling (nonzero λ_{De}/w_b) will be considered in our future work.

In summary, we have recalled the kinetic description of electron plasma waves carrying OAM in paraxial approximation and studied the wave propagation for a Maxwellian plasma by introducing a suitable variable transformation. A general representation of solution of the Vlasov–Poisson equations as a superposition of orthogonal LG modes is assumed. The dispersion and damping properties of twisted Langmuir mode in an electron–ion plasma are studied, and extension to an electron–positron plasma by defining an arbitrary mass parameter is discussed. Landau damping with modified resonance condition depends on the velocities in (v_θ, v_z) plane. The real wave frequency and the wave damping rate are derived by using the proposed variable transformation, which enabled us to evaluate the imaginary part of the susceptibility with velocity integral including only one pole, which contains axial and angular contributions. Thus, the method of obtaining wave damping by using the approach of decomposition (along z- and θ-directions) of the velocity integral involving two separate poles is improved. Due to the new presentation of the Landau integral, the integration space is extended and the limitation of the integration over a resonance line in the (v_z, v_θ) plane is removed. The corrected result of Ref. 17 is also examined numerically and compared to the present results. The analysis demonstrates the present formulation as a tool for smoother description of the propagation and damping of the twisted Langmuir mode in a kinetic framework.

DATA AVAILABILITY

The data that support the findings of this study are available within the article.

REFERENCES

[1] J. D. Jackson, *Classical Electrodynamics*, 2nd ed. (Wiley, New York, 1962).
[2] L. Allen, M. W. Beijersbergen, R. J. C. Spreeuw, and J. P. Woerdman, Phys. Rev. A **45**, 8185 (1992).
[3] H. Sroor, Y.-W. Huang, B. Sephton, D. Naidoo, A. Valles, V. Ginis, C.-W. Qiu, A. Ambrosio, F. Capasso, and A. Forbes, Nat. Photonics **14**, 498 (2020).
[4] M. Uchida and A. Tonomura, Nature **464**, 737 (2010).
[5] C. Jia, D. Ma, A. F. Schraffer, and J. Berakda, Nat. Commun. **10**, 2077 (2019).
[6] N. Bozinovic, Y. Yue, Y. Ren, M. Tur, P. Kristensen, H. Huang, A. E. Willner, and S. Ramachandran, Science **340**, 1545 (2013).
[7] J. T. Mendonca, B. Thide, and U. Then, Phys. Rev. Lett. **102**, 185005 (2009).
[8] J. T. Mendonca, S. Ali, and B. Thide, Phys. Plasmas **16**, 112103 (2009).
[9] J. T. Mendonca, Plasma Phys. Controlled Fusion **54**, 124031 (2012).
[10] J. Vieira, R. M. G. M. Trines, E. P. Alves, R. A. Fonseca, J. T. Mendona, R. Bingham, P. Norreys, and L. O. Silva, Phys. Rev. Lett. **117**, 265001 (2016).
[11] J. Vieira, R. M. G. M. Trines, E. P. Alves, R. A. Fonseca, J. T. Mendonca, R. Bingham, P. Norreys, and L. O. Silva, Nat. Commun. **7**, 10371 (2016).
[12] J. Verbeeck, H. Tian, and P. Schattschneider, Nature **467**, 301 (2010).

Published under an exclusive license by AIP Publishing

[13]P. K. Shukla, J. Geophys. Res. **118**, 1, https://doi.org/10.1029/2012JA018247 (2013).
[14]J. Vieira, J. T. Mendonca, and F. Quere, Phys. Rev. Lett. **121**, 054801 (2018).
[15]T. B. Leyser, L. Norin, M. McCarrick, T. R. Pedersen, and B. Gustavsson, Phys. Rev. Lett. **102**, 065004 (2009).
[16]M. Katoh, M. Fujimoto, H. Kawaguchi, K. Tsuchiya, K. Ohmi, T. Kaneyasu, Y. Taira, M. Hosaka, A. Mochihashi, and Y. Takashima, Phys. Rev. Lett. **118**, 094801 (2017).
[17]J. T. Mendonca, Phys. Plasmas **19**, 112113 (2012).
[18]S. A. Khan, Aman-ur-Rehman, and J. T. Mendonca, Phys. Plasmas **21**, 092109 (2014).
[19]J. D. Rodrigues, H. Tercas, and J. T. Mendonca, Europhys. Lett. **113**, 13001 (2016).
[20]D. R. Blackman, R. Nuter, P. Korneev, and V. T. Tikhonchuk, Phys. Rev. E **100**, 013204 (2019).
[21]J. Vieira and J. T. Mendonca, Phys. Rev. Lett. **112**, 215001 (2014).
[22]P. K. Shukla and B. Eliasson, J. Plasma Phys. **76**, 887 (2010).
[23]G. Sarri, K. Poder, J. Cole, W. Schumaker, A. D. Piazza, B. Reville, T. Dzelzainis, D. Doria, L. Gizzi, G. Grittani *et al.*, Nat. Commun. **6**, 6747 (2015).
[24]G. Sarri, M. E. Dieckmann, I. Kourakis, A. D. Piazza, B. Reville, C. H. Keitel, and M. Zepf, J. Plasma Phys. **81**, 455810401 (2015).
[25]G. P. Zank and R. G. Greaves, Phys. Rev. E **51**, 6079 (1995).
[26]M. R. Edwards, N. J. Fisch, and J. M. Mikhailova, Phys. Rev. Lett. **116**, 015004 (2016).

Published under an exclusive license by AIP Publishing